On the Modeling of Bearing Voltage and Current in PWM Converter-fed Electric Machines Using Electromagnetic Finite Element Analysis

Peng Han[1,*], *Senior Member, IEEE*, Yibin Zhang[1], *Student Member, IEEE*, Murat G. Kesgin[1], *Student Member, IEEE*, Greg Heins[2], *Member, IEEE*, Dean Patterson[2], *Life Fellow, IEEE*, Mark Thiele[2], *Member, IEEE*, and Dan M. Ionel[1], *Fellow, IEEE*

[1]SPARK Laboratory, ECE Department, University of Kentucky, Lexington, KY, USA
[2]Regal Beloit Corporation, Australia, Rowville, VIC 3178, Australia

peng.han@ieee.org, yibin.zhang@uky.edu, murat.kesgin@uky.edu, greg.heins@regalbeloit.com, dean.patterson@regalbeloit.com, mark.thiele@regalbeloit.com, dan.ionel@ieee.org

***Abstract*—Bearing voltages and resulting currents in electric machines driven by PWM converters with fast switching and high dv/dt can cause premature bearing failures. With the transition from conventional Si devices to wide bandgap (WBG) devices and increase in switching frequency, bearing voltages and currents become more significant and need to be addressed from the early design stage. This paper proposes to use coupled field-circuit electromagnetic finite element analysis (FEA) to model bearing voltage and current in electric machines, which takes into account the influence of distributed winding conductors and frequency-dependent winding RL parameters. The three known bearing current types are explained and modeled in a unified way by using the proposed approach with simple calculation examples. Potential bearing current issues in axial-flux machines, and possibilities of computation time reduction, are also discussed.**

***Index Terms*—Bearing voltage, bearing current, finite element analysis, computation time reduction, wide bandgap devices, electric machines.**

I. Introduction

Pulse width modulation (PWM) converters have pulsed voltage outputs featuring high dv/dt (voltage gradient) and high switching frequencies. The sum of the three-phase voltages is not zero and results in the common mode voltage (CMV), whose waveform depends on the DC bus voltage, modulation strategy, and the switching frequency.

The high dv/dt of the CMV at winding terminals introduces displacement currents flowing through not only the bearing lubricant but also winding insulations, which further results in varying flux encirculating the machine shaft. The circular flux around the shaft may introduce bearing currents that flow in both bearings in the drive and non-drive end, depending on the housing structure. For example, the 12-slot 10-pole (12s10p) permanent magnet synchronous machine (PMSM) shown in Fig. 1 has a cup-shaped external rotor structure and therefore there is no closed flowing path for this type of bearing current. Instead, the bearing current caused by the CMV and machine-related capacitors is the dominating component, as shown by the measured waveforms in Fig. 2 from the PMSM illustrated in Fig. 1.

Without appropriate counter-measures for these effects, a machine bearing can be destroyed within a few months of operation. Bearing failures caused by bearing currents account for approximately 9% in the cement industry [1]. A growing number of bearing current induced premature bearing failures have been reported, calling for more research effort into bearing currents and the associated mitigation techniques [2]. More recently, advanced wide band gap (WBG) devices based machine drives with higher switching frequencies ranging from a few hundreds of kHz to MHz and higher dv/dt pose new challenges for bearing reliability [3]. Unless otherwise stated, "bearing current" in this paper refer to PWM converter induced high-frequency bearing currents.

The main contributions of this paper include: proposing a coupled field-circuit finite element analysis (FEA) modeling approach for bearing voltage and current study in electric machines to take into account the influence of distributed winding conductors and frequency dependency of winding resistance and inductance; explaining and modeling of three known bearing current types based on the distributed-element circuit representation of electric machines and developed models in a unified way; exploring methods for computation time reduction.

The rest of this paper is organized as follows. Section II reviews bearing current issues in PWM converter fed electric machines and the main bearing current types. Section III presents the proposed modeling approach of bearing voltage and current based on electromagnetic FEA. Section IV examplifies the application of the proposed approach in analyzing main bearing types. Section V discusses the potential reduction of computation time and Section VI concludes the full paper.

[*]Dr. Peng Han was with the SPARK Laboratory, ECE Department, University of Kentucky, Lexington, KY and is now with Ansys Inc., San Jose, CA USA.

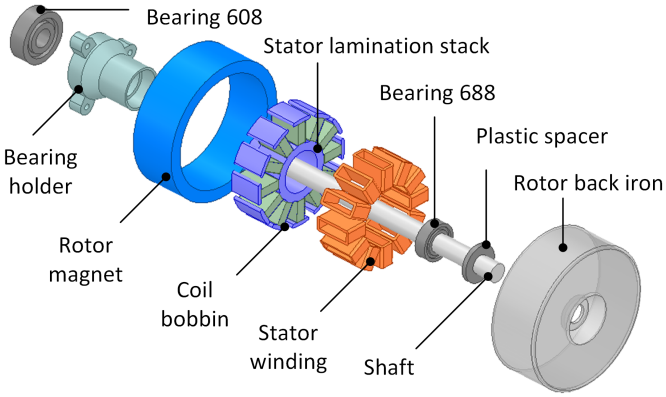

Fig. 1: Exploded view of the construction of a 12s10p PMSM example, which has a cup-shaped outer PM rotor and therefore has no conductive path for the circulating bearing current. The non-circulating type and ground leakage current still exist.

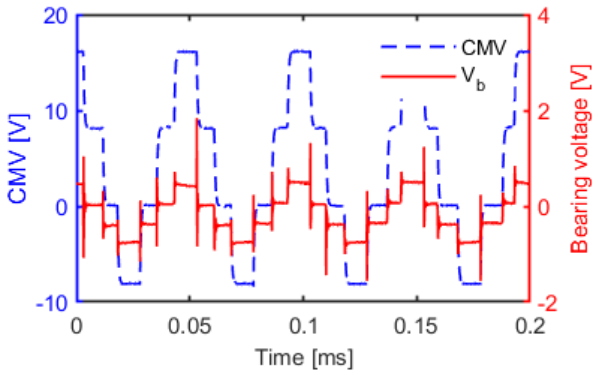

Fig. 2: Measured bearing voltage and CMV for the 12s10p PMSM shown in Fig. 1 at 2,400r/min using steel ball bearing. Overshoots of bearing voltage can be observed.

II. Bearing Current Issue in PWM Converter Fed Electric Machines

The voltage across the bearing lubricant film in steel ball bearings, i.e., the bearing voltage v_b, can be built up by the electrostatic charge accumulation, the CMV through capacitive coupling, and the circular flux created by displacement currents through the winding insulations or magnetic asymmetry via inductive coupling. Bearing current occurs when the bearing voltage is high enough to overcome the breakdown voltage of the lubricant. In case of ceramic bearings, the situation is different. The bearing current, once occurs, will flow through and damage the surface of bearing raceways, leading to premature bearing failures.

High-frequency bearing current types mainly include: the non-circulating bearing current caused by the shaft-to-frame voltage [4], the circulating type introduced by the shaft end-to-end voltage [5], and the leakage current to the ground [6]. The bearing voltage becomes a commonly-used indicator of bearing failures since all of these bearing current types depend on whether the voltage across the bearing is larger than the break-down value [2, 4]. Main bearing current flowing paths are illustrated in Fig. 3.

III. Modeling Approach Based on Electromagnetic FEA

The accurate modeling of bearing voltage and current in electric machines that can take into account the distribution of winding conductors (turns), frequency dependency of winding RL parameters, and variation of bearing capacitance is in great need. Existing studies mainly focus on the steady state value of bearing voltages in radial-flux machines, i.e., the bearing voltage to CMV ratio, and model the bearing voltages using equivalent circuit for frequency-domain analysis. The frequency-dependent winding RL parameters extracted from eddy-current solvers cannot fully capture the real-time variations and therefore this approach encounters difficulties in accurate time-domain dynamic analysis.

A coupled field-circuit electromagnetic finite element analysis (FEA) and experimental measurement based approach for the modeling of bearing voltage and current has been presented in [7] [8]. The schematic diagram of the model shown in Fig. 4 well illustrates the workflow. Each individual turn or a couple of adjacent turns can be modeled by a Π- or Γ-shaped circuit element. The capacitances are calculated from 2D or 3D elestrostatic FEA.

Through detail comparison study, the authors have demonstrated that when the coupled external circuit is distributed enough, i.e., with a sufficiently large number of turns, the predicted bearing voltages are the same no matter whether the Π- or Γ-shaped circuit element is used. A typical example of the external circuit for bearing voltage and current study following this approach is visualized in Fig. 5. For clarity and faster calculations, only capacitors with a coupling coefficient no smaller than 0.05 are included, which correspond to the triangular regions in Fig. 5. To be more general and to reduce the modeling time, the external circuit can be edited using scripts to describe the connection between electrical nodes.

IV. Application of Proposed Approach in Analyzing Main Bearing Types

A. Non-circulating Bearing Current

With inact bearing lubricant film, the bearing voltage v_b produced by the capacitive coupling is a function of the CMV at the winding terminals v_{com}, whose waveform mainly depends on the modulation scheme as shown in [9] [10]. In steady state, the bearing voltage can be written concisely as:

$$v_b \text{ (steady)} = \frac{C_{wr}}{C_{wr} + C_{sr} + (C_{b,DE} + C_{b,NDE})} v_{com}, \quad (1)$$

where C_{wr} is the total capacitance between windings and rotor core, C_{sr} the total capacitance between stator and rotor cores, $C_{b,DE}$ and $C_{b,NDE}$ bearing capacitances at the drive end and non-driven end, respectively. It should be noted that, the rising and falling of CMV also introduce some transients in bearing voltages, as shown in Fig. 2, which has not been fully considered in previous studies.

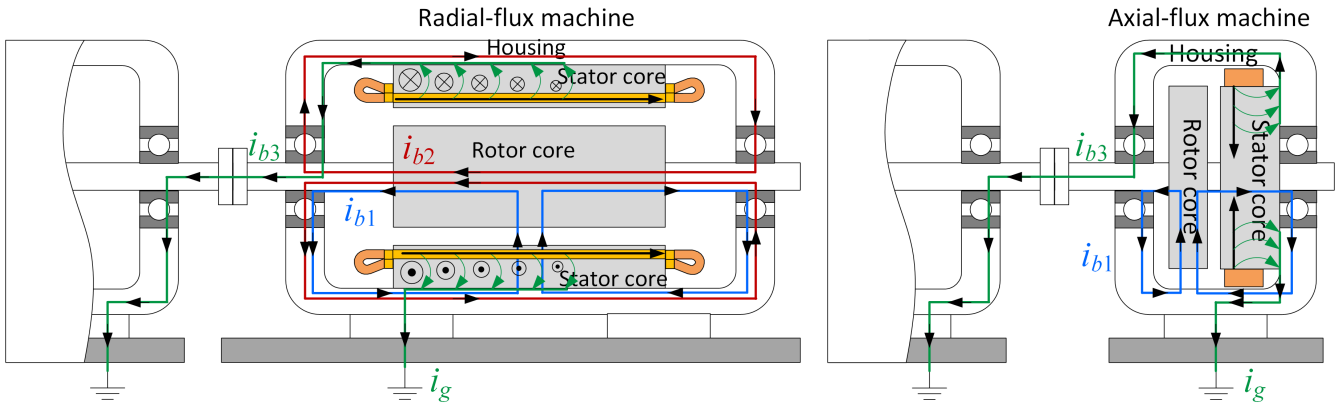

(a) **(b)**

Fig. 3: Flowing paths of bearing currents in: (a) radial-flux PM machines, (b) axial-flux PM machines. i_{b1} represents non-circulating bearing current, i_{b2} refers circulating bearing current, and i_{b3} is leakage current to the ground.

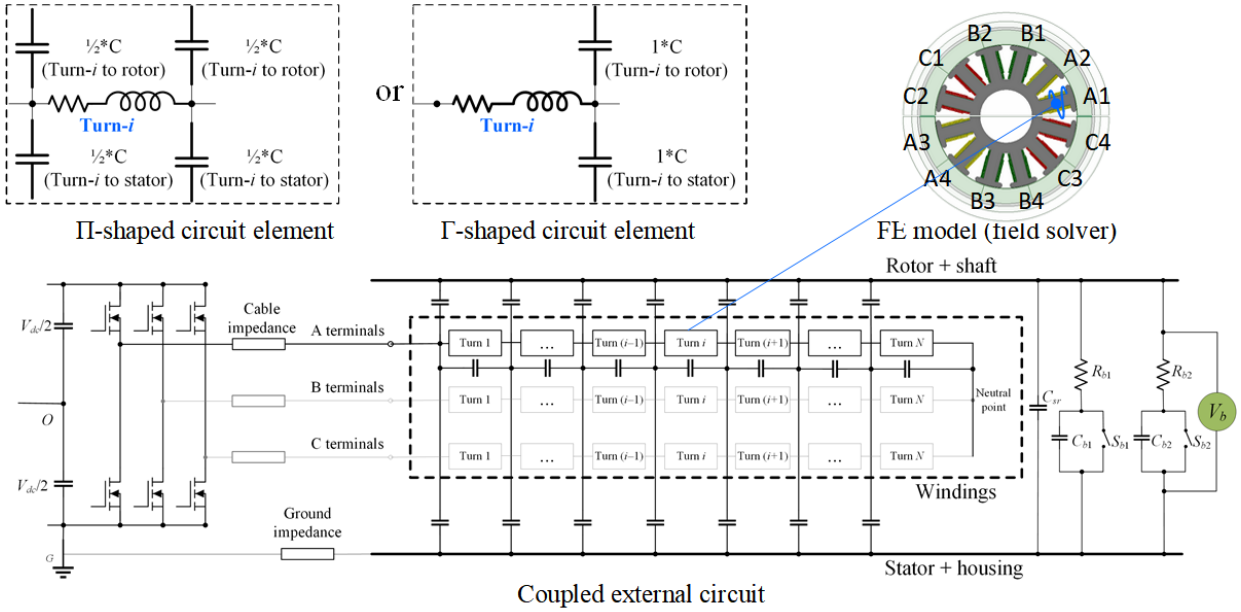

Fig. 4: The proposed modeling approach for bearing voltage and current based on coupled field-circuit electromagnetic FEA and experimental measurements. The details of winding turns are included in the FEA model. The connection of winding turns and the capacitors are included in the coupled external circuit. The bearing capacitances are measured from experiments using the approach presented in [7]. The FE model and coupled external circuit are solved together step by step to get the waveforms of bearing voltages, bearing currents, and voltage stress distribution in winding turns.

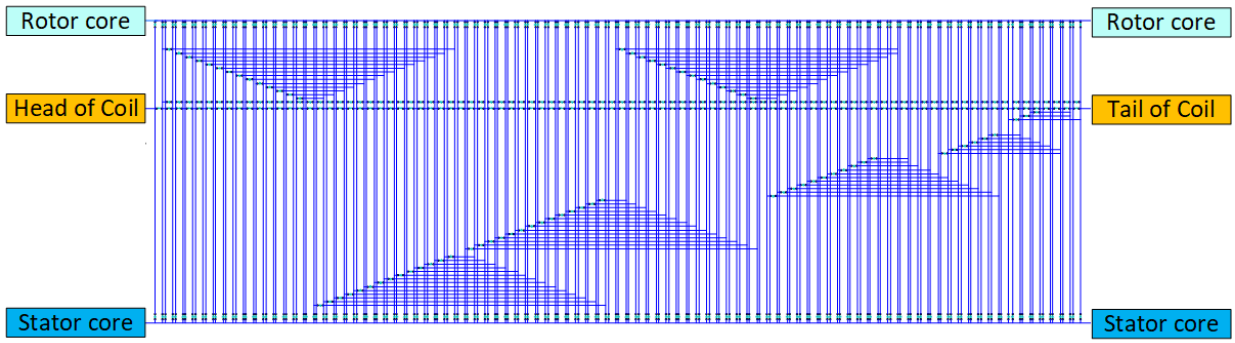

Fig. 5: Example of the coupled external circuit segment for one coil with 92 turns. Capacitors with coupling coefficients lower than 0.05 are not shown in the circuit for simplicity.

It has been well known that, according to (1), the steady-state bearing voltage mirrors CMV. With the proposed modeling approach, it has been found that even in steady state, the bearing voltage to CMV ratio is related to the winding capacitances and frequency dependent, as shown in Fig. 6. Observations in [11] also confirm this frequency dependency. When the instantaneous bearing voltage is large enough to break down the lubricant film, the bearing current flow through the breakdown point and its amplitude will be determined by the overall voltage and impedance along the flowing path denoted by blue lines in Fig. 3.

B. Circulating Bearing Current

The high dv/dt at the winding terminals causes additional displacement currents mainly flowing into the stator core through the winding insulation due to the winding-to-stator-core capacitance C_{ws}. The frequencies of these currents range from a few kHz to several MHz. These currents excite a circular magnetic flux around the machine shaft similar to that introduced by magnetic asymmetries, which further induces a shaft end-to-end voltage v_{sh}, which can be calculated by:

$$v_{sh}(t) = -\frac{d\psi_{cir}}{dt} = -\frac{d}{dt}\int_0^{2\pi}\int_0^{Ro} B_t(r,\theta,t)L_{stk}drd\theta, \tag{2}$$

where ψ_{cir} is the circular flux around the shaft, R_o the radius of the selected region for calculation, $B_t(r,\theta,t)$ the tangential component of the flux density as a function of radius r, angle θ and time t, L_{stk} the stack length.

To quantify the circular flux around the shaft and the introduced shaft end-to-end voltage using electromagnetic FEA, the rotor center of a 12s10p PMSM was adjusted to provided some eccentricity. The flux contour under loaded condition with rotor eccentricity shows some asymmetry. By using (2), the shaft end-to-end voltage v_{sh} can be obtained, as shown in Fig. 7. Specifically $V_{sh} = 0$ indicates the shaft end-to-end voltage without rotor eccentricity.

Similar to the magnetic asymmetry introduced by rotor eccentricity, the displacement currents through the winding insulation lead to a non-zero net current in the machine cross section and consequently created similar circular flux ψ_{cir} and shaft end-to-end voltage. By incorporating this voltage into the model illustrated in Fig. 4, the circulating bearing current can also be taken into account.

If v_{sh} is large enough to break down the lubricant films of the drive-end bearing and non-drive-end bearing, a circulating type bearing current will flow along the loop "housing - non-drive end - shaft - drive end" [5], as denoted by red lines in Fig. 3. Therefore, the bearing currents in the drive-end and non-drive-end bearings are of the opposite directions, whose amplitude depends on the shaft end-to-end voltage induced by the circulating flux and the overall impedance of flowing path.

C. Ground Leakage Current

The capacitive currents produced by the high dv/dt at the winding terminals mentioned in Section IV-B may flow partly as the rotor-to-ground leakage current through the bearings if

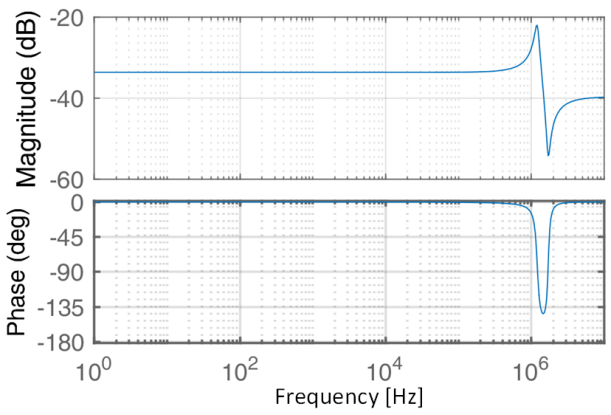

Fig. 6: Frequency dependency of bearing voltage to CMV ratio showing the importance of predicting bearing current transients at varied frequencies (non-circulating type).

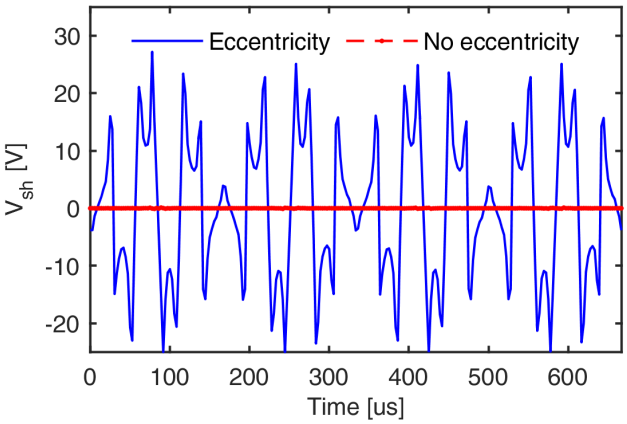

Fig. 7: Shaft voltage waveforms v_{sh} in a 12s10p PMSM with 1mm static rotor eccentricity and without rotor eccentricity. The amplitude depends on the eccentricity and rotor speed (circulating type).

the rotor of the machine under study or the load machine is grounded and has a significantly lower impedance path than the grounding of its housing, as denoted by green lines in Fig. 3. A typical example for the rotor-to-ground leakage current via the driven machine has been presented in [6]. This type of bearing current is caused by the impedance difference between possible flowing paths so it is inherently modeled once all the components, such as grounding and supplying cables, driven machines, couplers, etc, are included.

In radial-flux machines, all of the three types of bearing current may occur, and their flowing paths have been illustrated in Fig. 3a. For axial-flux machines, the non-circulating bearing current and ground leakage current exist. there is still no clear evidence on whether there is the circulating bearing current in axial-flux machines, which needs more careful examination. Therefore, only the flowing paths of the non-circulating current and ground leakage current are plotted in the axial-flux machine shown in Fig. 3b.

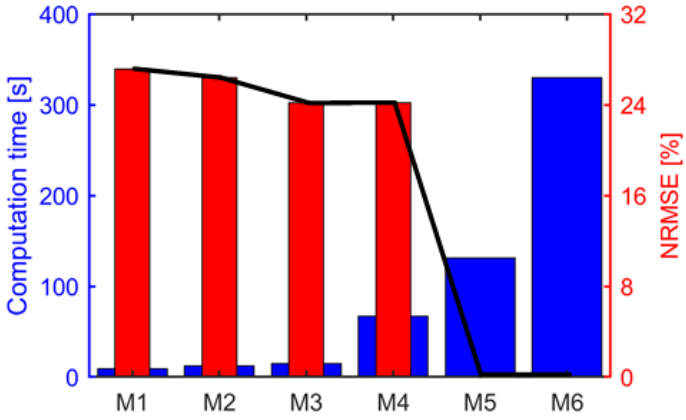

Fig. 8: Computation time and NRMSE for models. M1 – 92 turns per FE coil; M2, M3, M4 and M5 – 46, 23, 4, and 2 turns per FE coil, respectively; M6 – 1 turn per FE coil.

V. Discussion on Potential Reduction of Computation time

The proposed method has a high fidelity in terms of the bearing voltage and current calculations, but at the same time, requires large computational efforts since it involves the detailed modeling of winding turns and predicts the voltage and current in very fine time steps (ns level) and long time intervals (μs level) to capture the fast transients. Therefore, the potential reduction of model complexity and computation time is also necessary.

One effective approach to reducing the computation time is to reduce the number of turns in the coupled external circuit because the time-stepping scheme used in this paper requires multiple FEA calculations to extract the resistance and inductance matrices for each time step. A comparison of 6 models in terms of computation time and normalized root mean square error (NRMSE) is plotted in Fig. 8, showing the feasibility of this approach. NRMSE is defined as:

$$NRMSE = \frac{RMSE}{\bar{O}}, \tag{3}$$

where $\bar{O}$ is the average value from the baseline model. RMSE is the root mean square error, and it can be calculated by:

$$RMSE = \sqrt{\frac{\sum_{i=1}^{n}(X_{b,i} - X_{m,i})^2}{n}}, \tag{4}$$

where $X_{b,i}$ and $X_{m,i}$ are values from the baseline model and studied model, respectively. n is the number of temporal data points. In the example shown in Fig. 8, M6 is the baseline model and all the other models are compared with it.

With two real turns represented by 1 turn in the coupled circuit, the computation time is reduced from 330s to 131s without losing the accuracy. Other approaches, including optimizing the time-stepping scheme, optimzing the number of real turns per circuit coil, simplifying the external circuit by neglecting the insignificant capacitors, using adaptive time step size, etc., are the main directions for future study.

VI. Conclusion

This paper proposes to use electromagnetic FEA to model bearing voltage and current in electric machines to better consider the effect of distributed winding turns and frequency dependence of winding RL parameters. By examining the distributed-element equivalent circuit representation of electric machines, more specifically, the PMSM, it is shown that all the three known bearing current types in machines driven by PWM converters can be derived once the distributed capacitors are considered. It is also shown that the reduction of computation time is possible by grouping multiple real winding turns into one FE coil without reducing the accuracy. Bearing voltages and currents in different machine types, such as PMSMs, squirrel-cage induction machines, slip-ring doubly-fed induction machines, and wound-field synchronous machines, will be different, but can be studied using the examplified modeling approach based on electromagnetic FEA. More work on further reducing the computation time of the FEA based modeling approach and its application in evaluating the bearing current mitigation using recommended common practices are under way.

Acknowledgment

The support of Regal Beloit Corporation, University of Kentucky, the L. Stanley Pigman Endowment, and of Ansys Inc., is gratefully acknowledeged.

References

[1] R. Hoppler and R. A. Errath, "ABB motor bearings," *Global Cement Magazine*, Oct. 2007.

[2] A. Muetze and A. Binder, "Practical rules for assessment of inverter-induced bearing currents in inverter-fed AC motors up to 500 kW," *IEEE Trans. Ind. Electron.*, vol. 54, no. 3, pp. 1614–1622, 2007.

[3] A. von Jouanne, R. Collin, M. Stephens, Y. Miao, B. Thayil, C. Li, E. Agamloh, and A. Yokochi, "Motor bearing current characterization in SiC-based variable frequency drive applications," in *Proc. IEEE Energy Convers. Congr. Expo. (ECCE)*, 2020, pp. 2718–2725.

[4] D. Busse, J. Erdman, R. J. Kerkman, D. Schlegel, and G. Skibinski, "Bearing currents and their relationship to PWM drives," *IEEE Trans. Power Electron.*, vol. 12, no. 2, pp. 243–252, March 1997.

[5] Shaotang Chen, T. A. Lipo, and D. W. Novotny, "Circulating type motor bearing current in inverter drives," in *Rec. IEEE Ind. Appl. Soc. Annu. Meeting*, vol. 1, Oct. 1996, pp. 162–167.

[6] J. Ollila, T. Hammar, J. Iisakkala, and H. Tuusa, "On the bearing currents in medium power variable speed AC drives," in *in Proc. Int. Electr. Mach. Drives Conf. (IEMDC)*, 1997, pp. MD1/1.1–MD1/1.3.

[7] P. Han, G. Heins, D. Patterson, M. Thiele, and D. M. Ionel, "Evaluation of bearing voltage reduction in electric machines by using insulated shaft and bearings," in *Proc. IEEE Energy Convers. Congr. Expo. (ECCE)*, 2020, pp. 5584–5589.

[8] P. Han, G. Heins, D. Patterson, M. Thiele, and D. M. Ionel, "Modeling of bearing voltage in electric machines based on electromagnetic fea and measured bearing capacitance," *IEEE Transactions on Industry Applications*, pp. 1–1, 2021.

[9] BALDOR, "Electric discharge machining damage and how it affects bearings," June 2021. [Online]. Available: https://www.motionindustries.com/knowledgelinks/bearings

[10] O. A. Mohammed, S. Ganu, N. Abed, S. Liu, and Z. Liu, "High frequency pm synchronous motor model determined by FE analysis," *IEEE Trans. Mag.*, vol. 42, no. 4, pp. 1291–1294, 2006.

[11] M. Yea, J. Kim, and K. J. Han, "Frequency-dependent bearing voltage model for squirrel-cage induction motors," *IEEE Transactions on Industrial Electronics*, pp. 1–1, 2021.